

Stimulated Raman scattering in the degenerate regime

Yao Zhao¹, Suming Weng^{2,3}, Zhengming Sheng^{2,3,4}, and Jianqiang Zhu^{1,3}

¹Key Laboratory of High Power Laser and Physics, Shanghai Institute of Optics and Fine Mechanics, Chinese Academy of Sciences, Shanghai 201800, China

²Key Laboratory for Laser Plasmas (MoE), School of Physics and Astronomy, Shanghai Jiao Tong University, Shanghai 200240, China

³Collaborative Innovation Center of IFSA (CICIFSA), Shanghai Jiao Tong University, Shanghai 200240, China

⁴SUPA, Department of Physics, University of Strathclyde, Glasgow G4 0NG, UK

Abstract

Stimulated Raman scattering (SRS) in plasma in the degenerate regime is studied theoretically and numerically. Different from normal SRS with the non-degenerate eigen electrostatic mode excited, the degenerate SRS is developed at plasma density $n_e > 0.25n_c$ when the laser amplitude is larger than a certain threshold. To satisfy the phase-matching conditions of frequency and wavenumber, the excited electrostatic mode has a constant frequency around half of the incident light frequency $\omega_0/2$, which is no longer the non-degenerate eigenmode of electron plasma wave ω_{pe} . Both the scattered light and the electrostatic wave are trapped in plasma with their group velocities being zero. Super hot electrons are produced by the degenerate electrostatic wave. Our theoretical model is validated by particle-in-cell simulations. The SRS driven in this degenerate regime is an important laser energy loss mechanism in the laser plasma interactions as long as the laser intensity is higher than 10^{15}W/cm^2 .

Keywords: Laser plasma interactions; stimulated Raman scattering; hot electrons

1. Introduction

Laser plasma interactions (LPI) are widely associated with many applications, such as inertial confinement fusion (ICF)^[1–3], radiation sources^[4], plasma optics^[5,6], and laboratory astrophysics^[7,8]. The concomitant parametric instabilities found in LPI are nonlinear processes which can greatly affect the outcome^[9]. Generally, laser plasma instabilities^[10,11], especially stimulated Raman scattering (SRS), stimulated Brillouin scattering (SBS) and two-plasmon decay (TPD) instability, have been mainly considered in ICF with the incident laser intensity less than 10^{15}W/cm^2 ^[12–14]. However, the laser intensity may be in the order of 10^{16} or even 10^{17}W/cm^2 in shock ignition^[15–19], Brillouin amplification^[20,21], and the interactions of high power laser with matter^[22–24]. Therefore, the parametric instabilities close to the regime of subrelativistic intensity needs to be explored in depth.

As well known, SRS usually develops in plasma density not larger than the quarter critical density $n_e \leq 0.25n_c$ due to the decay of the scattering light in its propagation in the overdense density plasma^[4,10]. In the density region $n_e \leq$

$0.25n_c$, the electrostatic wave is the non-degenerate eigenmode of the electron plasma wave. Relativistic intensity lasers can reduce the effective electron plasma frequency, and therefore non-degenerate eigenmode SRS may develop at $n_e > 0.25n_c$ ^[25]. In this work, we show the presence of degenerate SRS, which is found at plasma density $n_e > 0.25n_c$ even without considering the relativistic effect. The development of degenerate electrostatic mode is described by the linear perturbations of fluid equations, which may lead to a few subsequent nonlinear phenomena^[20,26–28]. This mode develops only when the laser intensity exceeds a certain threshold. The theoretical model is supported by particle-in-cell (PIC) simulations.

2. Theoretical analysis of SRS in the degenerate regime

Generally, SRS is a three-wave instability that a laser decays into an electrostatic wave with frequency equal to the eigen electron plasma wave, and a light wave. However, the stimulated electrostatic wave is no longer the eigenmode of the electron plasma wave in the SRS degenerate regime, where both the frequencies of scattered light and electrostatic field are nearly half of the incident laser frequency. The

Correspondence to: Yao Zhao. Email: yaozhao@siom.ac.cn

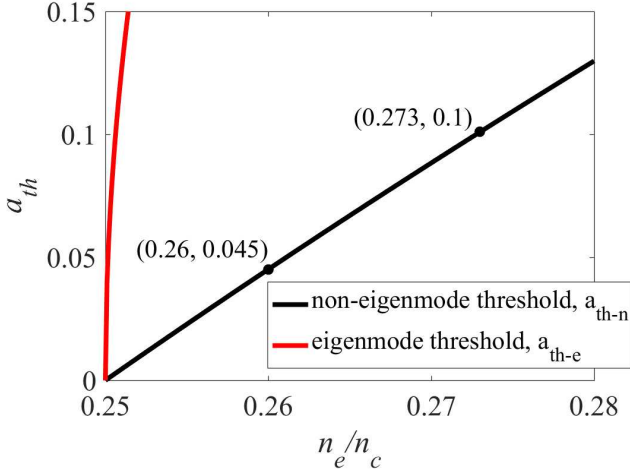


Figure 1. Amplitude thresholds for the development of non-degenerate eigenmode and degenerate SRS in plasma above the quarter critical density. The threshold for the case of non-degenerate eigenmode SRS a_{th-e} is due to the relativistic effect.

mechanism of this instability can be described by the SRS dispersion relation at plasma density $n_e > 0.25n_c$.

To investigate the degenerate SRS mechanism in laser plasma interactions, we firstly introduce the nonrelativistic dispersion relation of SRS in cold plasma^[10]

$$\omega_e^2 - \omega_{pe}^2 = \frac{\omega_{pe}^2 k_e^2 c^2 a_0^2}{4} \left(\frac{1}{D_{e+}} + \frac{1}{D_{e-}} \right), \quad (1)$$

where $D_{e\pm} = \omega_e^2 - k_e^2 c^2 \mp 2(k_0 k_e c^2 - \omega_0 \omega_e)$, and a_0 is the laser normalized amplitude. The relation between laser intensity I and a_0 is given by $I(\text{W/cm}^2) = 1.37 \times 10^{18} a_0^2 / [\lambda(\mu\text{m})]^2$. Also in Eq. (1), ω_0 and ω_e are the frequencies of incident laser and electrostatic wave, respectively. k_0 and k_e are respectively the wavenumbers of pump laser and electrostatic wave. Generally, we have $\text{Re}(\omega_e) = \omega_{pe}$ in the SRS non-degenerate eigenmode regime $n_e \leq 0.25n_c$. However, when the amplitude of incident laser a_0 larger than a threshold, stimulated degenerate electrostatic mode $\text{Re}(\omega_e) \neq \omega_{pe}$ will be developed at $n_e > 0.25n_c$.

Now we analytically solve Eq. (1) under $n_e > 0.25n_c$. Let $\omega_e = \omega_{er} + i\omega_{ei}$, where ω_{er} and ω_{ei} are the real and imaginary part of ω_e , respectively. The wavenumber of scattering light is a real $k_{sc} = 0$ in the degenerate regime, i.e., the scattered light is trapped in the plasma. And to keep the phase-matching conditions, we set the electrostatic wavenumber $k_e c = k_0 c$. In this case, the imaginary part of Eq. (1) can be simplified to

$$(\omega_0 \omega_{ei} - 2\omega_{ei} \omega_{er})(\omega_{ei}^2 - \omega_{er}^2 - 2\omega_0 \omega_{er} + 3\omega_0^2 - 3\omega_{pe}^2)(\omega_{er}^2 + \omega_{ei}^2 - \omega_{er} \omega_0 - \omega_{pe}^2) = 0. \quad (2)$$

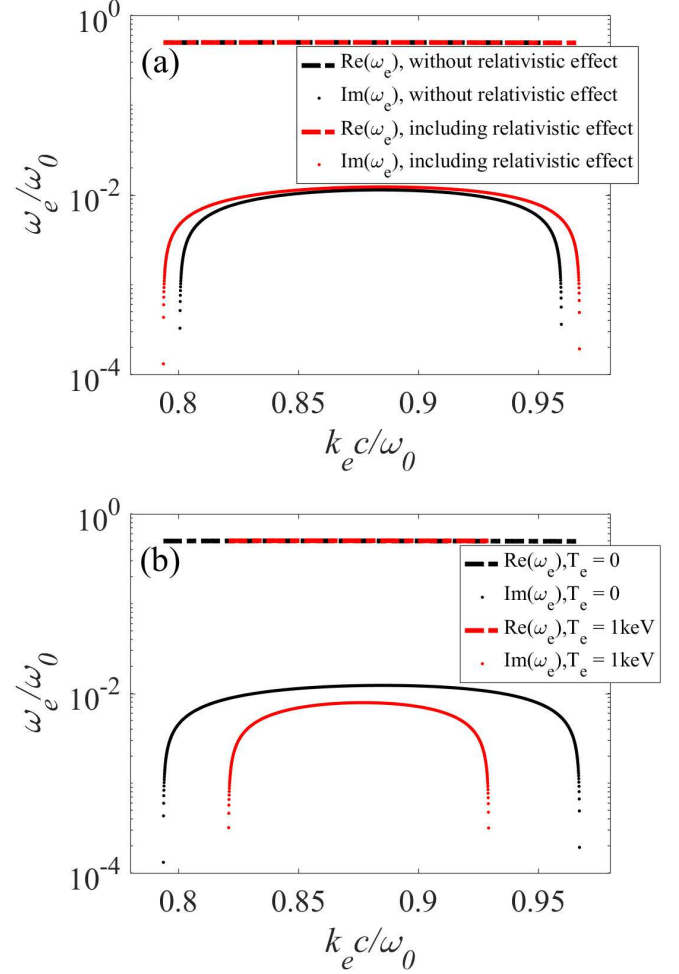


Figure 2. Numerical solutions of SRS dispersion equation at plasma density $n_e = 0.27n_c$ with laser amplitude $a_0 = 0.1$. (a) The relativistic modification on the degenerate SRS at $T_e = 0$. (b) The effect of electron temperature on degenerate SRS. The dotted line and dashed line are the imaginary part and the real part of the solutions, respectively.

Equation (2) is satisfied for any ω_{pe} when $\omega_{er} = \omega_0/2$. Therefore, the frequency of the electrostatic wave is a constant, and is independent of the plasma density. The phase velocity of the electrostatic wave is around $v_{ph} = \omega_{er}/k_e \gtrsim c/\sqrt{3} \sim 0.58c$.

Substituting $\omega_{er} = \omega_0/2$ into the real part of Eq. (1), one obtains the growth rate of degenerate SRS

$$\omega_{ei} = \frac{1}{2} \sqrt{4\omega_{pe}(\omega_0 - \omega_{pe}) + \omega_{pe}^2 a_0^2 k_0^2 c^2 / \omega_0^2 - \omega_0^2}. \quad (3)$$

The above equation indicates that the growth rate ω_{ei} is reduced by the increasing of plasma density. The threshold a_{th-n} for SRS developing in the degenerate regime can be obtained from $4\omega_{pe}(\omega_0 - \omega_{pe}) + \omega_{pe}^2 a_{th-n}^2 k_0^2 c^2 / \omega_0^2 - \omega_0^2 \gtrsim 0$,

i.e.,

$$a_{th-n} \gtrsim \frac{\omega_0 \sqrt{\omega_0^2 + 4(\omega_{pe}^2 - \omega_{pe}\omega_0)}}{\omega_{pe}k_0c}. \quad (4)$$

Equation (4) indicates that $0.25n_c$ is the turning point between non-degenerate eigenmode SRS and degenerate SRS, where the threshold $a_{th-n} = 0$.

For the density region just near the quarter critical density $n_e \gtrsim 0.25n_c$, Eq. (4) can be simplified to $a_{th-n} \gtrsim (8/\sqrt{3})(n_e/n_c - 0.25)$. Therefore, the condition for the excitation of degenerate SRS in a plasma with density $n_e \gtrsim 0.25n_c$ is that the amplitude of pump laser satisfies the above condition, which is almost linearly proportional to the plasma density.

In the following, we consider the relativistic modification of the SRS degenerate in hot plasma. The dispersion of SRS under the relativistic intensity laser is^[9,25]

$$\omega_e^2 - \omega_L^2 = \frac{\omega_{pe}^2 k_e^2 c^2 a_0^2}{4\gamma^2} \left(\frac{1}{D_{e+}} + \frac{1}{D_{e-}} \right), \quad (5)$$

where $\omega_L^2 = \omega_{pe}^2 + 3k_e^2 v_{th}^2$ with $\omega_{pe}' = \omega_{pe}/\sqrt{\gamma}$, $\gamma = (1 + a_0^2/2)^{1/2}$ and v_{th} are the relativistic factor and electron thermal velocity, respectively. Different from degenerate SRS, the threshold for non-degenerate eigenmode SRS developing in cold plasma with $n_e > 0.25n_c$ is $\omega_{pe}' \leq 0.5\omega_0$, i.e., $a_{th-e} \geq \sqrt{2(16n_e^2/n_c^2 - 1)}$. As a comparison, the driven amplitudes for degenerate SRS a_{th-n} and non-degenerate eigenmode SRS a_{th-e} at different plasma densities are shown in Fig. 1. One finds that the amplitude threshold for non-degenerate eigenmode SRS is much larger than degenerate SRS, i.e., $a_{th-e} \gg a_{th-n}$. Therefore, the intensity of SRS in $n_e > 0.25n_c$ is underestimated according to the previous eigenmode model. As an example, the threshold for laser driving degenerate SRS at plasma density $n_e = 0.26n_c$ is around $a_{th-n} = 0.045$. A laser with amplitude $a_0 = 0.1$ can develop degenerate SRS in the plasma region with density $0.25n_c < n_e \leq 0.273n_c$.

Following the similar steps of the non-relativistic case, the imaginary part of Eq. (5) is simplified to

$$(\omega_0\omega_{ei} - 2\omega_{ei}\omega_{er})(\omega_{ei}^2 - \omega_{er}^2 - 2\omega_0\omega_{er} + 3\omega_0^2 - 3\omega_{pe}^2)(\omega_{er}^2 + \omega_{ei}^2 - \omega_{er}\omega_0 - \omega_L^2) = 0. \quad (6)$$

We obtain the same identical relation for the real part $\omega_{er} = \omega_0/2$ from Eq. (6). Note that the relativistic factor and electron temperature has no effect on ω_{er} which is no longer the non-degenerate eigen frequency ω_L . The dispersion relation of the degenerate electrostatic mode satisfies

$$\omega_{er} = \frac{\omega_0}{2} = \frac{1}{2} \sqrt{(k_e^2 c^2 + \omega_{pe}^2)}. \quad (7)$$

From Eq. (7) we know that the group velocity of degenerate

electrostatic wave is $v_g = \delta\omega_{er}/\delta k_e \approx 0$. Therefore, electrostatic wave will be trapped in the plasma.

The comparisons between the numerical solutions of Eqs. (1) and (5) are exhibited in Fig. 2. One finds that $\text{Re}(\omega_e) = \omega_0/2$ is a constant even including relativistic and temperature effects. The frequency of electron plasma wave is reduced by the relativistic factor $\omega_{pe}' = \omega_{pe}/\sqrt{\gamma}$. Therefore, the growth rate ω_{ei} is increased by the relativistic modification as shown in Fig. 2(a). On the contrary, the frequency of electron plasma wave is enhanced by the electron temperature $\omega_L = \sqrt{\omega_{pe}^2 + 3k_e^2 v_{th}^2}$, and therefore we find a decrease of the growth rate at higher temperature $T_e = 1\text{keV}$ in Fig. 2(b). Note that the above studies are discussed in the weak relativistic regime, where the plasma density modulation induced by the laser ponderomotive force is weak.

Phase-matching conditions are satisfied in the SRS degenerate regime, therefore the frequency of concomitant light is also $\text{Re}(\omega_s) \approx 0.5\omega_0$, which can be obtained from the dispersion relation of scattered light

$$\omega_s^2 - k_s^2 c^2 - \omega_{pe}^2 = D_{s+} + D_{s-}, \quad (8)$$

where $D_{s\pm} = \omega_{pe}^2 (k_s \pm k_0)^2 c^2 a_0^2 / 4[(\omega_s \pm \omega_0)^2 - \omega_{pe}^2]$.

According to the linear parametric model of inhomogeneous plasma, the Rosenbluth gain saturation coefficient for convective instability is $G = 2\pi\Gamma^2/v_s v_p K'^{[29]}$, where Γ , v_s and v_p are instability growth rate, group velocity of scattering light and plasma wave, respectively. K is the wavenumber mismatch for incident light, scattering light and plasma wave. As it is known, convective instability transits to absolute instability when $K = 0$ ^[30]. Based on the above discussions, the mismatching term of degenerate SRS is $K_{ne} = k_0 - k_e - k_s = 0$ due to $k_e = k_0$ and $k_s = 0$ all the time. Therefore, degenerate SRS is an absolute instability in inhomogeneous plasma.

In conclusion, different from normal SRS, a new type of degenerate SRS can develop in plasma with density $n_e > 0.25n_c$. The stimulated electrostatic mode has an almost constant frequency around half of the incident light frequency $\omega_0/2$, which is no longer the non-degenerate eigenmode of the electron plasma wave ω_{pe} . The group velocities of concomitant light and electrostatic wave are zero in the degenerate regime. The degenerate SRS develops only when the laser intensity is higher than a certain threshold which is related to the plasma density.

3. Simulations for degenerate SRS excitation

3.1. 1D simulations for degenerate SRS in homogeneous plasma

To validate the analytical predictions for degenerate SRS, we have performed several one-dimensional (1D) simulations by using the OSIRIS code^[31,32]. The space and time given in the following are normalized by the laser wavelength in

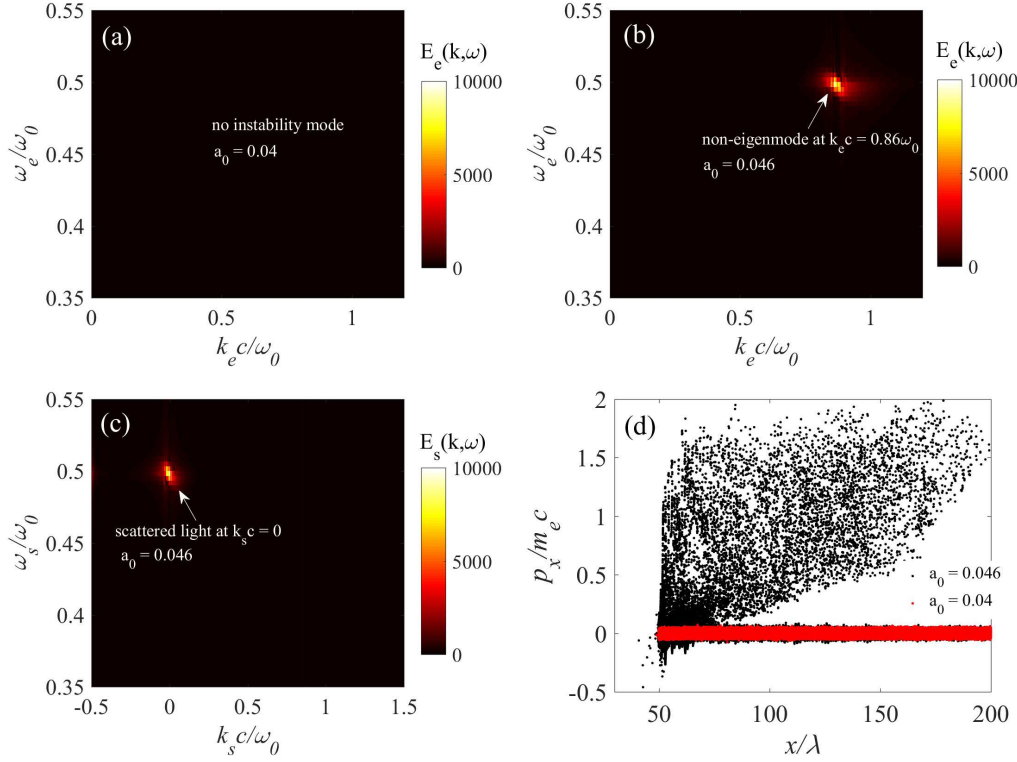


Figure 3. Distributions of the electrostatic wave in (k_e, ω_e) space obtained for the time window $[100, 400]\tau$ at plasma density $n_e = 0.26n_c$ under (a) pump laser amplitude $a_0 = 0.04$ and (b) pump laser amplitude $a_0 = 0.046$. (c) Distribution of the electromagnetic wave in (k_s, ω_s) space obtained under the same conditions of (b). (d) Longitudinal phase space distribution of electrons under different laser amplitudes at $t = 600\tau$.

vacuum λ and the laser period τ . A linearly-polarized semi-infinite pump lasers with a uniform amplitude is incident from the left boundary of the simulation box. In this subsection, only the fluid property of the instability is considered, therefore we set electron temperature $T_e = 100\text{eV}$ with immobile ions. The plasma density is $n_e = 0.26n_c$.

Based on Eq. (4) and Fig. 1 we know that the triggering threshold for degenerate SRS is $a_{th-n} = 0.045$ at density $n_e = 0.26n_c$. To validate the theoretical threshold, two simulation examples under different laser intensities are displayed here. Figure 3(a) shows the case when the laser amplitude is less than the threshold ($a_0 = 0.04 < 0.045$), and no instability mode can be found. When the laser amplitude is increased to $a_0 = 0.046 > 0.045$, the degenerate electrostatic mode can be found at $k_e c \approx 0.86\omega_0$ and $\omega_e \approx 0.499\omega_0$ in Fig. 3(b). The corresponding electromagnetic mode with $k_s c \approx 0$ and $\omega_s \approx 0.5\omega_0$ is shown in Fig. 3(c). These simulation results agree well with the analytical prediction. As discussed above, the phase velocity of the degenerate electrostatic wave is around $v_{ph} \sim 0.58c$ at $n_e = 0.26n_c$. Therefore, numbers of electrons are heated enormously at the nonlinear stage $t \gtrsim 600\tau$ in the SRS degenerate regime as compared to the case below the threshold as shown in Fig. 3(d).

3.2. 2D simulations for degenerate SRS in homogeneous plasma

To further validate the linear development and nonlinear evolution of degenerate SRS in high-dimensionality with mobile ions, we have performed several two-dimensional (2D) simulations. The plasma occupies a longitudinal region from 25λ to 125λ and a transverse region from 5λ to 25λ with homogeneous density $n_e = 0.26n_c$. The initial electron temperature is $T_e = 100\text{eV}$. Ions are movable with mass $m_i = 3672m_e$ and an effective charge $Z = 1$. A s-polarized (electric field of light is perpendicular to the simulation plane) semi-infinite pump laser with a peak amplitude $a_0 = 0.05$ at focal plane $x = 75\lambda$ is incident from the left boundary of the simulation box.

According to Eq. (4), we know that the incident laser with peak amplitude $a_0 = 0.05$ is sufficient to develop degenerate SRS at plasma density $n_e = 0.26n_c$. The simulation results for plasma density $n_e = 0.26n_c$ are displayed in Figs. 4(a)-4(d). Fourier transform of the electrostatic wave is taken for the time window $[320, 480]\tau$. We summate the Fourier spectrum along the transverse direction between $y = 14.4\lambda$ and $y = 15.6\lambda$, and show the distribution in Fig. 4(a). One can find a degenerate electrostatic mode around $k_e c = 0.86\omega_0$ and $\omega_e = 0.492\omega_0$. Note that the growth rate of SBS is about half of the degenerate SRS, therefore, SBS have little

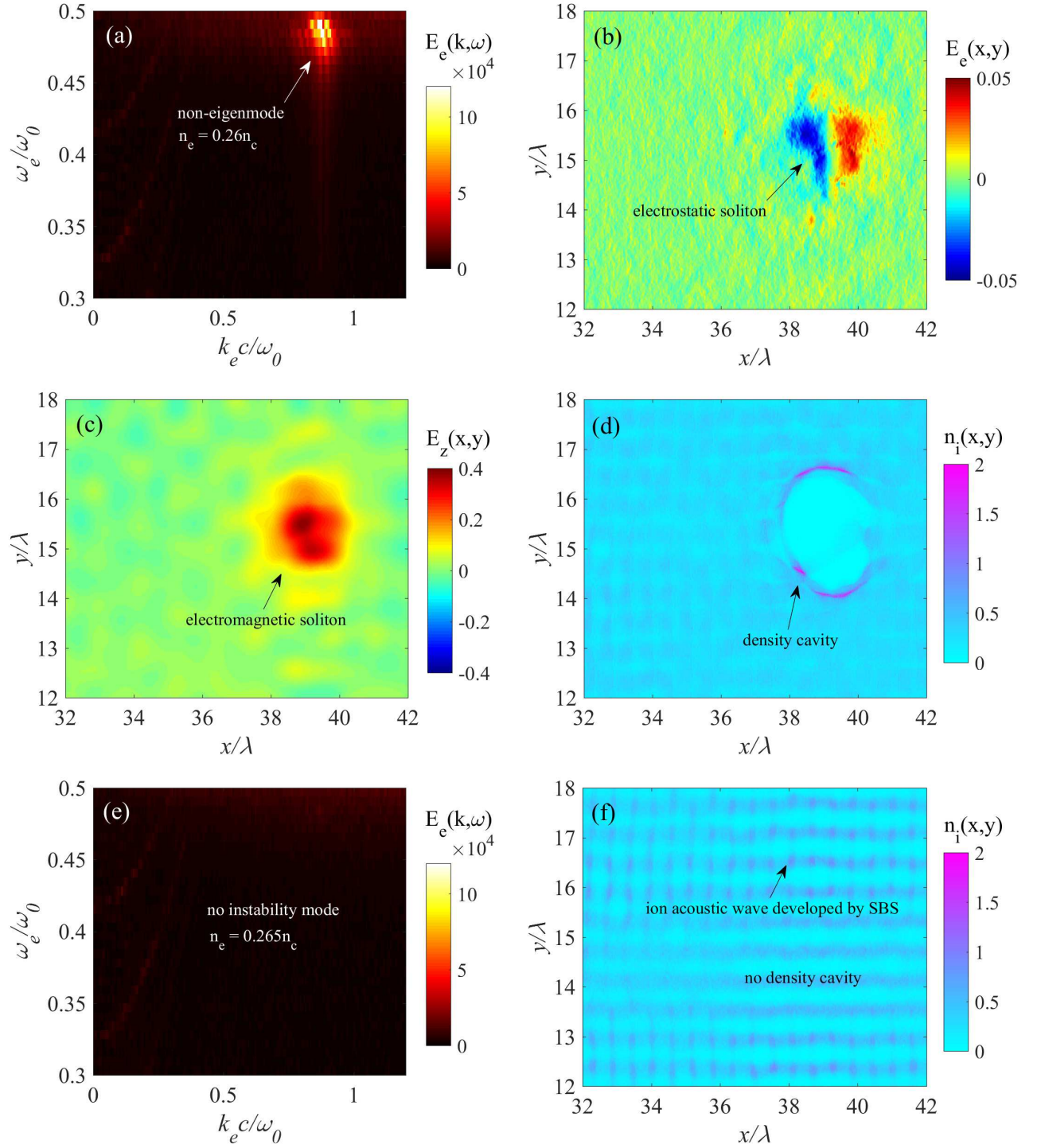


Figure 4. The plasma density is $n_e = 0.26n_c$ for (a)-(d). (a) Distribution of the electrostatic wave in (k_e, ω_e) space obtained for the time window $[320, 480]\tau$ and transverse region $[14.4, 15.6]\lambda$. (b) Spatial distribution of electrostatic wave at $t = 1850\tau$. (c) Spatial distribution of electromagnetic wave at $t = 1850\tau$. (d) Spatial distribution of ion density at $t = 1950\tau$. The plasma density is $n_e = 0.265n_c$ for (e)-(f). (e) Distribution of the electrostatic wave in (k_e, ω_e) space obtained for the time window $[320, 480]\tau$ and transverse region $[14.4, 15.6]\lambda$. (f) Spatial distribution of the ion density at $t = 1950\tau$. E_e and E_z are normalized by $m_e \omega_0 c/e$, where m_e and e respectively are the electron mass and electron charge. n_i is normalized by n_c .

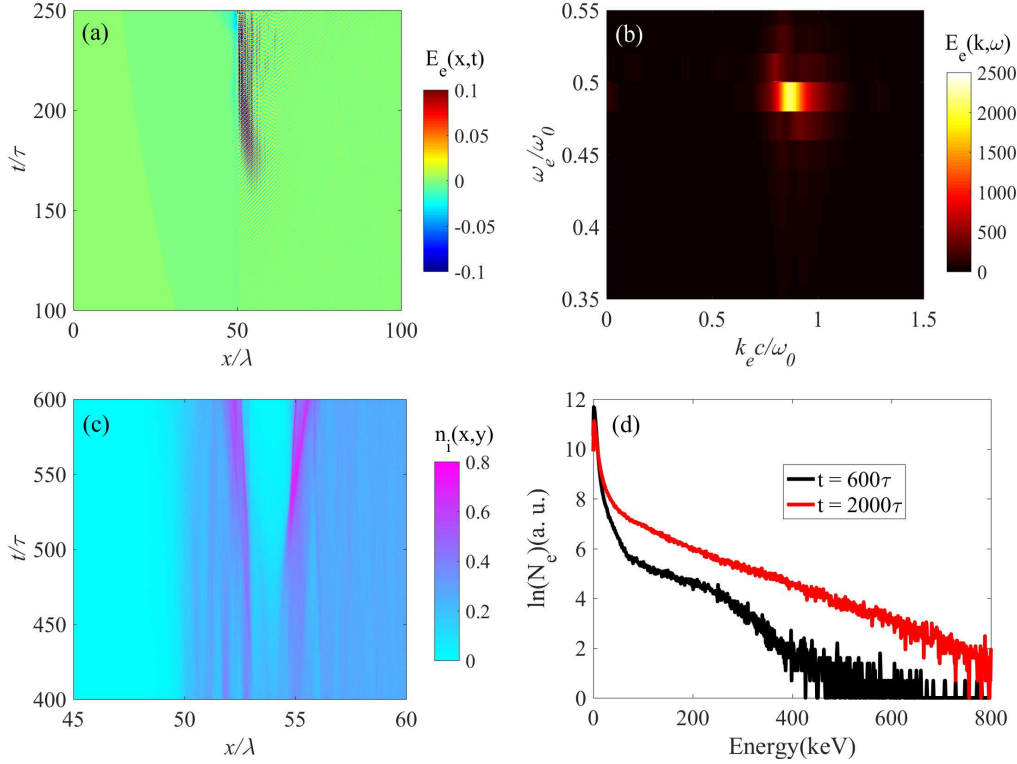


Figure 5. (a) The spatial-temporal distributions of electrostatic wave. (b) Distributions of the electrostatic wave in (k_e, ω_e) space obtained for the time window $[150, 200]\tau$. (c) The spatial-temporal distributions of ion density. (d) Energy distributions of electrons at different times. E_e and n_i respectively are normalized by $m_e \omega_0 c/e$ and n_c .

effect on the development of degenerate SRS. As discussed in Sec. 2, the group velocities of the electrostatic wave and electromagnetic wave associated with the degenerate SRS are zero. As a result, they will be trapped in the plasma. This is confirmed in our numerical simulation as shown in Figs. 4(b) and 4(c), the electrostatic wave and the concomitant electromagnetic wave form localized structures. The trapped light and electrostatic wave may cause the laser energy deficit in ICF related experiments^[33]. The trapped waves expel the ions to form density cavity at later time $t = 1950\tau$ as seen from Fig. 4(d). These plasma cavities subsequently affect the evolution of the degenerate SRS and SBS^[20,27,28]. Note that this density cavity is formed due to the degenerate SRS, which is different from the solitons generated by relativistic intensity lasers^[34–38].

The laser with peak amplitude $a_0 = 0.05 < a_{th-n} = 0.067$ is insufficient to develop degenerate SRS at $n_e = 0.265n_c$. The simulation results under plasma density $n_e = 0.265n_c$ are displayed in Figs. 4(e) and 4(f). The comparison between Figs. 4(a) and 4(e) indicates that the pump laser with peak amplitude $a_0 = 0.05$ fails to drive degenerate SRS at $n_e = 0.265n_c$ when the amplitude threshold is not reached. Only the ion acoustic wave developed by SBS with wavenumber $k_i c = 2k_0 c = 1.72\omega_0$ can be found in Fig. 4(f). And no density cavities has been formed under this conditions. These results further indicate

that degenerate SRS is a seed for the subsequent nonlinear physical phenomena.

3.3. 1D simulations for degenerate SRS in inhomogeneous plasma

To study the degenerate SRS in hot inhomogeneous plasma, we have performed a simulation for the inhomogeneous plasma $n_e = 0.26 \exp[(x - 50)/1000]n_c$ with density range $[0.26, 0.287]n_c$. The plasma locates in $x = [50, 150]\lambda$, and two 50λ vacuums are left on either side of the plasma. The initial electron temperature is $T_e = 2\text{keV}$. Ions are movable with mass $m_i = 3672m_e$. The ion charge and temperature respectively are $Z = 1$ and $T_i = 1\text{keV}$. The driving laser is a linearly-polarized semi-infinite pump lasers with a uniform amplitude $a_0 = 0.07$.

The spatial-temporal evolution of electrostatic wave is exhibited in Fig. 5(a). We find that a strong electrostatic wave has been developed at the front of plasma $x \lesssim 60\lambda$ at $t = 180\tau$. The electrostatic wave envelop is found to be stationary due to its group velocity $v_g = 0$. Note that the spatial gradient has little effect on the development of degenerate SRS, by reason that the phase matching of the three waves is always satisfied in inhomogeneous plasma. Therefore, degenerate SRS is an absolute instability. Figure 5(b) shows the distribution of electrostatic wave in (k_e, ω_e)

space, where one can find a spectrum around $\omega_e = 0.499\omega_0$. This result further validates that the frequency of degenerate electrostatic wave is independent of plasma density and electron temperature. The electrostatic and electromagnetic wave trapped in plasma will expel ions. From Fig. 5(c) we know that ion density cavity is gradually formed from $t = 400\tau$ at the front of plasma. Large numbers of hot electrons are produced by the degenerate electrostatic field as shown in Fig. 5(d). As discussed above, the phase velocity of the degenerate electrostatic field is around $0.58c$. The temperature of the electron hot tail at $t = 2000\tau$ is around 141keV. The transmission rate of the pump laser through plasma is about 19.46% at $t = 2000\tau$, which indicate that degenerate SRS is an important pump energy loss mechanism in the laser plasma interactions as long as the laser intensity is higher than 10^{15}W/cm^2 .

4. Summary

In summary, we have shown theoretically and numerically that the degenerate SRS develops at plasma density $n_e > 0.25n_c$ when the laser amplitude is larger than a certain threshold. The electrostatic wave produced by the degenerate SRS has a constant frequency $\omega_0/2$, which is no longer the non-degenerate eigen electron plasma wave ω_{pe} . The phase velocity of the degenerate electrostatic wave is about $0.58c$, which corresponds to the electron energy of 175keV. Therefore, super hot electrons can be produced via the development of the degenerate SRS. The trapped electromagnetic wave and electrostatic wave associated with this instability can drive density cavities in plasma. Our theoretical model is validated by PIC simulations. The degenerate SRS is an important pump energy loss mechanism in the laser plasma interactions as long as the laser intensity higher than 10^{15}W/cm^2 .

5. Acknowledgement

This work was supported by the Natural Science Foundation of Shanghai (No. 19YF1453200), the National Natural Science Foundation of China (Nos. 11775144 and 1172109), and the Strategic Priority Research Program of Chinese Academy of Sciences (Grant Nos. XDA25050800 and XDA25050100). The authors would like to acknowledge the OSIRIS Consortium, consisting of UCLA and IST (Lisbon, Portugal) for providing access to the OSIRIS 4.0 framework.

References

1. E. M. Campbell, V. N. Goncharov, T. C. Sangster, S. P. Regan, P. B. Radha, R. Betti, J. F. Myatt, D. H. Froula, M. J. Rosenberg, and I. V. Igumenshchev, *Laser-direct-drive program: Promise, challenge, and path forward*, Matter Radiat. Extrem. **2**, 37 (2017).
2. D. Froula, L. Divol, R. London, R. Berger, T. Döppner, N. Meezan, J. Ralph, J. Ross, L. Suter, and S. Glenzer, *Experimental basis for laser-plasma interactions in ignition hohlraums at the National Ignition Facility*, Phys. Plasmas **17**, 056302 (2010).
3. J. F. Myatt, J. Zhang, R. W. Short, A. V. Maximov, W. Seka, D. H. Froula, D. H. Edgell, D. T. Michel, I. V. Igumenshchev, D. E. Hinkel, P. Michel, and J. D. Moody, *Multiple-beam laser-plasma interactions in inertial confinement fusion*, Phys. Plasmas **21**, 055501 (2014).
4. L. C. S., T. V. K., and E. B., *High-power laser-plasma interaction* (Cambridge University Press, 2019).
5. L. Lancia, A. Giribono, L. Vassura, M. Chieramello, C. Riconda, S. Weber, A. Castan, A. Chatelain, A. Frank, and T. Gangolf, *Signatures of the Self-Similar Regime of Strongly Coupled Stimulated Brillouin Scattering for Efficient Short Laser Pulse Amplification*, Phys. Rev. Lett. **116**, 075001 (2016).
6. G. Lehmann and K. H. Spatschek, *Nonlinear Brillouin amplification of finite-duration seeds in the strong coupling regime*, Phys. Plasmas **20**, 073112 (2013).
7. R. P. Drake, *High-energy-density physics: fundamentals, inertial fusion, and experimental astrophysics* (Springer Science and Business Media, 2006).
8. K. Falk, *Experimental methods for warm dense matter research*, High Power Laser Sci. Eng. **6**, e59 (2018).
9. P. Gibbon, *Short pulse laser interactions with matter* (World Scientific Publishing Company, 2004).
10. W. L. Kruer, *The physics of laser plasma interactions*, Vol. 70 (Addison-Wesley New York, 1988).
11. D. S. Montgomery, *Two decades of progress in understanding and control of laser plasma instabilities in indirect drive inertial fusion*, Phys. Plasmas **23**, 055601 (2016).
12. R. S. Craxton, K. S. Anderson, T. R. Boehly, V. N. Goncharov, D. R. Harding, J. P. Knauer, R. L. McCrory, P. W. McKenty, D. D. Meyerhofer, J. F. Myatt, *et al.*, *Direct-drive inertial confinement fusion: A review*, Phys. Plasmas **22**, 110501 (2015).
13. J. Lindl, O. Landen, J. Edwards, and E. Moses, *Review of the national ignition campaign 2009-2012*, Phys. Plasmas **21**, 020501 (2014).
14. J. D. Moody, B. J. MacGowan, J. E. Rothenberg, R. L. Berger, L. Divol, S. H. Glenzer, R. K. Kirkwood, E. A. Williams, and P. E. Young, *Backscatter reduction using combined spatial, temporal, and polarization beam smoothing in a long-scale-length laser plasma*, Phys. Rev. Lett. **86**, 2810 (2001).
15. R. Betti and O. A. Hurricane, *Inertial-confinement fusion with lasers*, Nat. Phys. **12**, 435 (2016).
16. D. Batani, S. Baton, A. Casner, S. Depierreux, M. Hohenberger, O. Klimo, M. Koenig, C. Labaune, X. Ribeyre, C. Rousseaux, G. Schurtz, W. Theobald,

- and V. Tikhonchuk, *Physics issues for shock ignition*, Nucl. Fusion **54**, 054009 (2014).
17. G. Cristoforetti, L. Antonelli, D. Mancelli, S. Atzeni, F. Baffigi, F. Barbato, D. Batani, G. Boutoux, F. D'Amato, J. Dostal, and et al., *Time evolution of stimulated Raman scattering and two-plasmon decay at laser intensities relevant for shock ignition in a hot plasma*, High Power Laser Sci. Eng. **7**, e51 (2019).
 18. O. Klimo, S. Weber, V. T. Tikhonchuk, and J. Limpouch, *Particle-in-cell simulations of laser-plasma interaction for the shock ignition scenario*, Plasma Phys. Control. Fusion **52**, 055013 (2010).
 19. Y. J. Gu, O. Klimo, P. Nicola, S. Shekhanov, S. Weber, and V. T. Tikhonchuk, *Collective absorption of laser radiation in plasma at sub-relativistic intensities*, High Power Laser Sci. Eng. **7**, e39 (2019).
 20. S. Weber, C. Riconda, and V. T. Tikhonchuk, *Low-Level Saturation of Brillouin Backscattering due to Cavity Formation in High-Intensity Laser-Plasma Interaction*, Phys. Rev. Lett. **94**, 055005 (2005).
 21. L. Lancia, J. R. Marques, M. Nakatsutsumi, C. Riconda, S. Weber, S. Hüller, A. Mančić, P. Antici, V. T. Tikhonchuk, A. Héron, et al., *Experimental evidence of short light pulse amplification using strong-coupling stimulated Brillouin scattering in the pump depletion regime*, Phys. Rev. Lett. **104**, 025001 (2010).
 22. B. Rethfeld, D. S. Ivanov, M. E. Garcia, and S. I. Anisimov, *Modelling ultrafast laser ablation*, J. Phys. D: Appl. Phys. **50**, 193001 (2017).
 23. D. Price, R. More, R. Walling, G. Guethlein, R. Shepherd, R. Stewart, and W. White, *Absorption of ultrashort laser pulses by solid targets heated rapidly to temperatures 1-1000 eV*, Phys. Rev. Lett. **75**, 252 (1995).
 24. K. M. George, J. T. Morrison, S. Feister, G. K. Ngirmang, J. R. Smith, A. J. Klim, J. Snyder, D. Austin, W. Erbsen, K. D. Frische, and et al., *High-repetition-rate (\geq kHz) targets and optics from liquid microjets for high-intensity laser-plasma interactions*, High Power Laser Sci. Eng. **7**, e50 (2019).
 25. Y. Zhao, J. Zheng, M. Chen, L. L. Yu, S. M. Weng, C. Ren, C. S. Liu, and Z. M. Sheng, *Effects of relativistic electron temperature on parametric instabilities for intense laser propagation in underdense plasma*, Phys. Plasmas **21**, 112114 (2014).
 26. A. Ghizzo, T. W. Johnston, T. Réveillé, P. Bertrand, and M. Albrecht-Marc, *Stimulated-Raman-scatter behavior in a relativistically hot plasma slab and an electromagnetic low-order pseudocavity*, Phys. Rev. E **74**, 046407 (2006).
 27. C. F. Wu, Y. Zhao, S.-M. Weng, M. Chen, and Z.-M. Sheng, *Nonlinear evolution of stimulated scattering near $1/4$ critical density*, Acta Physica Sinica **68**, 195202 (2019).
 28. C. Riconda, S. Weber, V. Tikhonchuk, J.-C. Adam, and A. Heron, *Two-dimensional particle-in-cell simulations of plasma cavitation and bursty Brillouin backscattering for nonrelativistic laser intensities*, Physics of plasmas **13**, 083103 (2006).
 29. M. N. Rosenbluth, *Parametric instabilities in inhomogeneous media*, Phys. Rev. Lett. **29**, 565 (1972).
 30. C. S. Liu, M. N. Rosenbluth, and R. B. White, *Raman and Brillouin scattering of electromagnetic waves in inhomogeneous plasmas*, Phys. Fluids **17**, 1211 (1974).
 31. R. A. Fonseca, L. O. Silva, F. S. Tsung, V. K. Decyk, W. Lu, C. Ren, W. B. Mori, S. Deng, S. Lee, T. Katsouleas, and J. Dongarra, in *OSIRIS: A three-dimensional, fully relativistic particle in cell code for modeling plasma based accelerators*, International Conference on Computational Science (Springer, 2002) pp. 342–351.
 32. R. G. Hemker, *Particle-in-cell modeling of plasma-based accelerators in two and three dimensions*, arXiv preprint arXiv:1503.00276 (2015).
 33. Y. Zhao, Z. Sheng, S. Weng, S. Ji, and J. Zhu, *Absolute instability modes due to rescattering of stimulated Raman scattering in a large nonuniform plasma*, High Power Laser Sci. Eng. **7**, e20 (2019).
 34. T. Z. Esirkepov, F. F. Kamenets, S. V. Bulanov, and N. M. Naumova, *Low-frequency relativistic electromagnetic solitons in collisionless plasmas*, Jetp Letters **68**, 36 (1998).
 35. S. V. Bulanov, T. Z. Esirkepov, N. M. Naumova, F. Pegoraro, and V. A. Vshivkov, *Solitonlike Electromagnetic Waves behind a Superintense Laser Pulse in a Plasma*, Phys. Rev. Lett. **82**, 3440 (1999).
 36. Y. Sentoku, T. Z. Esirkepov, K. Mima, K. Nishihara, F. Califano, F. Pegoraro, H. Sakagami, Y. Kitagawa, N. M. Naumova, and S. V. Bulanov, *Bursts of Superreflected Laser Light from Inhomogeneous Plasmas due to the Generation of Relativistic Solitary Waves*, Phys. Rev. Lett. **83**, 3434 (1999).
 37. N. Naumova, S. Bulanov, T. Esirkepov, D. Farina, K. Nishihara, F. Pegoraro, H. Ruhl, and A. Sakharov, *Formation of Electromagnetic Postsolitons in Plasmas*, Phys. Rev. Lett. **87**, 185004 (2001).
 38. D. Wu, W. Yu, S. Fritzsche, C. Y. Zheng, and X. T. He, *Formation of relativistic electromagnetic solitons in over-dense plasmas*, Phys. Plasmas **26**, 063107 (2019).